International Veterinary Ultrasound Society (IVUSS) Suggested Abdominal Case Format
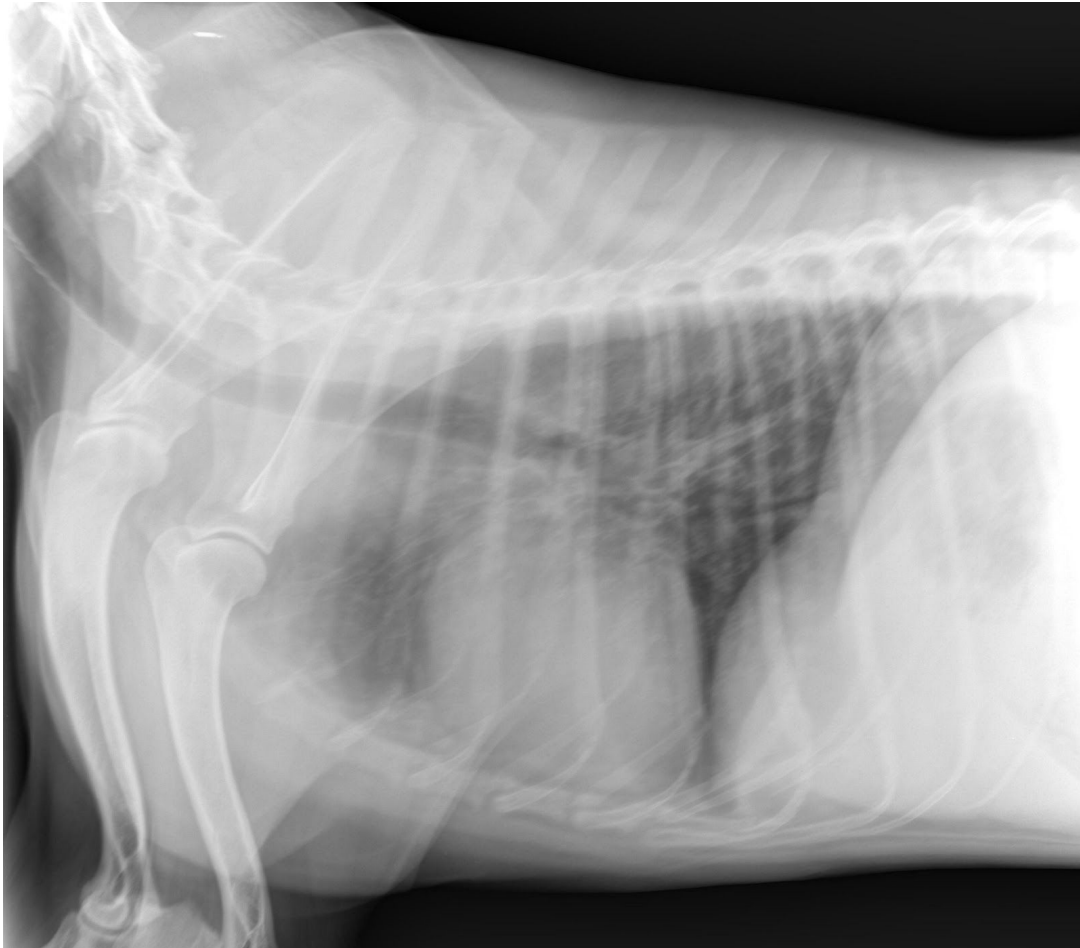
Basic Abdominal Case 5

Mila, a six years old neutered female Golden Retriever, is presented for a second opinion. One month ago her appetite started to decrease and at this moment she's not eating at all. During the past year Mila lost 11 kilograms. Since one week she shows bilateral third eyelid prolapse. Mila is not vomiting. Her stools were loose for the first time this morning. During the walks she's starting to cough which is also noted sometimes at night. No polyuria/polydipsia, no signs of nausea, no limping is noted. Forty days ago a tick has been removed. Two weeks ago a complete blood work was performed by the vet with no abnormalities detected. Lyme disease was tested 2 times with two weeks interval and was positive. Cytology of the mandibular lymph nodes was done but not diagnostic. Mila is on doxycycline 400 mg once a day since six weeks. Cimicoxib was added to the therapy but the last dose was given 5 weeks ago.

During clinical examination pale pink mucous membranes with a normal capillary refill time are detected. Auscultation is within normal limits and the tracheal reflex is negative. The femoral pulse is normal. Firm and clearly enlarged mandibular lymph nodes are palpated. A mild enlargement of the left prescapular and right popliteus lymph node is found. The remaining peripheral lymph nodes do not show any abnormalities. Abdominal palpation reveals splenomegaly and suspicion of hepatomegaly. Her rectal temperature (38.4°C) is normal. Mild muscle atrophy is present and a body condition score of 5/9 is given. Mila's ears are normal. Her eyes show bilateral protrusion of the third eyelid with some presence of mucopurulent discharge. The Schirmer tear test is bilateral lower than 5 mm after one minute. Mila's coat is dull and scales are present. Her weight is 29,55 kg.

Radiographic examination

The right lateral thoracic projection is of poor quality. Due to panting a motion artifact is present, blurring the thoracic spine and intrathoracic structures. The extrathoracic structures are within normal limits. The cardiac contours appear normal and a normal vertebral heart score is detected. The pulmonary parenchyma shows a normal opacity and the vasculature appears normal. No changes are seen at the level of the mediastinum, trachea and main bronchi.

Radiographic examination

A lateral projection of the abdomen shows hepatomegaly with the liver margins extending beyond the costal arch. Mild enlargement of the spleen although the margins still seem sharp. Little peritoneal detail is present in the midabdomen. No other abnormalities are detected.

Blood work

	Result	Reference range	Unit
Complete blood count			
RBC	5,5	5,65 - 8,87	x10^12/
HCT	35,2	37,3 - 61,7	%
HGB	13,2	13,1 - 20,5	g/dl
MCV	64	61,6 - 73,5	fL
MCH	24	21,2 - 25,9	pg
MCHC	37,5	32 - 37,9	g/dl
RDW	15,6	13,6 - 21,7	%
% RETIC	1,5		%
RETIC	84,2	10,0 - 110,0	K/µL
WBC	14,89	5,05 - 16,76	x10^9/L
NEU	10,54	2,95 - 11,64	x10^9/L
LYM	1,91	1,05 - 5,1	x10^9/L
MONO	2,33	0,16 - 1,12	x10^9/L
EOS	0,11	0,06 - 1,23	x10^9/L
BASO	0	0,00 - 0,10	x10^9/L
PLT	215	148 - 484	K/µL
Chemistry profile			
Glucose	5,71	4,11 - 7,95	mmol/L
Urea	2,5	2,5 - 9,6	mmol/L
Creatinine	55	44 - 159	µmol/L
BUN/CR	12		
Phosphate	1,93	0,81 - 2,2	mmol/L
Calcium	2,24	1,98 - 3,00	mmol/L
Total protein	53	52 - 82	g/L
Albumin	21	23 - 40	g/L
Globulin	32	25 - 45	g/L
Alb/glob	0,7		
ALT	347	10 - 125	U/L
ALKP	> 2000	23 - 212	U/L
GGT	39	0 - 11	U/L
Tbil	13	0 - 15	µmol/L
Cholesterol	13,42	2,84 - 8,26	mmol/L
Amylase	1177	500 - 1500	U/L
Lipase	1408	200 - 1800	U/L

Urine analysis

Specific gravity 1034

Sonographic examination

Ultrasound (Epic 5, Philips) examination was performed on the sedated patient in dorsal recumbency, using a curved array 9-2MHz probe and high frequency 7.5-10 MHz linear probe.

Transverse image of the right to mid portion of the liver. The hepatic parenchyma appears heterogeneous with a hyperechoic area in the near field and a more hypoechoic parenchyma in the far field. However, these changes disappear when using the linear probe. Transverse sections through the hepatic vessels are detected. The gallbladder is seen as a round structure containing hyperechoic sludge in the dependent portion of the bladder. The diaphragm-lung interface is seen as a hyperechoic line distally to the liver in the far field.

Sagittal image of the mid to left sided liver. Normal hypoechoic and homogeneous liver parenchyma with anechoic round cross sections through the hepatic vessels. The gastric fundus is shown on the right side of the liver containing some fluid and gas.

Sagittal image of the liver and gastric fundus, using the high frequency linear probe. A homogeneous hepatic parenchyma is demonstrated. The hyperechoic margins of the portal veins are well demarcated. Hypoechoic areas are detected in the liver due to artifact formation from the hyperechoic lesions in the near field. These hyperechoic lesions can be associated with calcified nodules or granulomas, fibrotic lesions, biliary calculi or focal steatosis. Hepatic ligaments may also create these kinds of artifacts.

Transverse image of the left sided liver showing a homogeneous and hypoechoic liver without nodular lesions. The portal veins are visible as tubular structures with a hyperechoic wall.
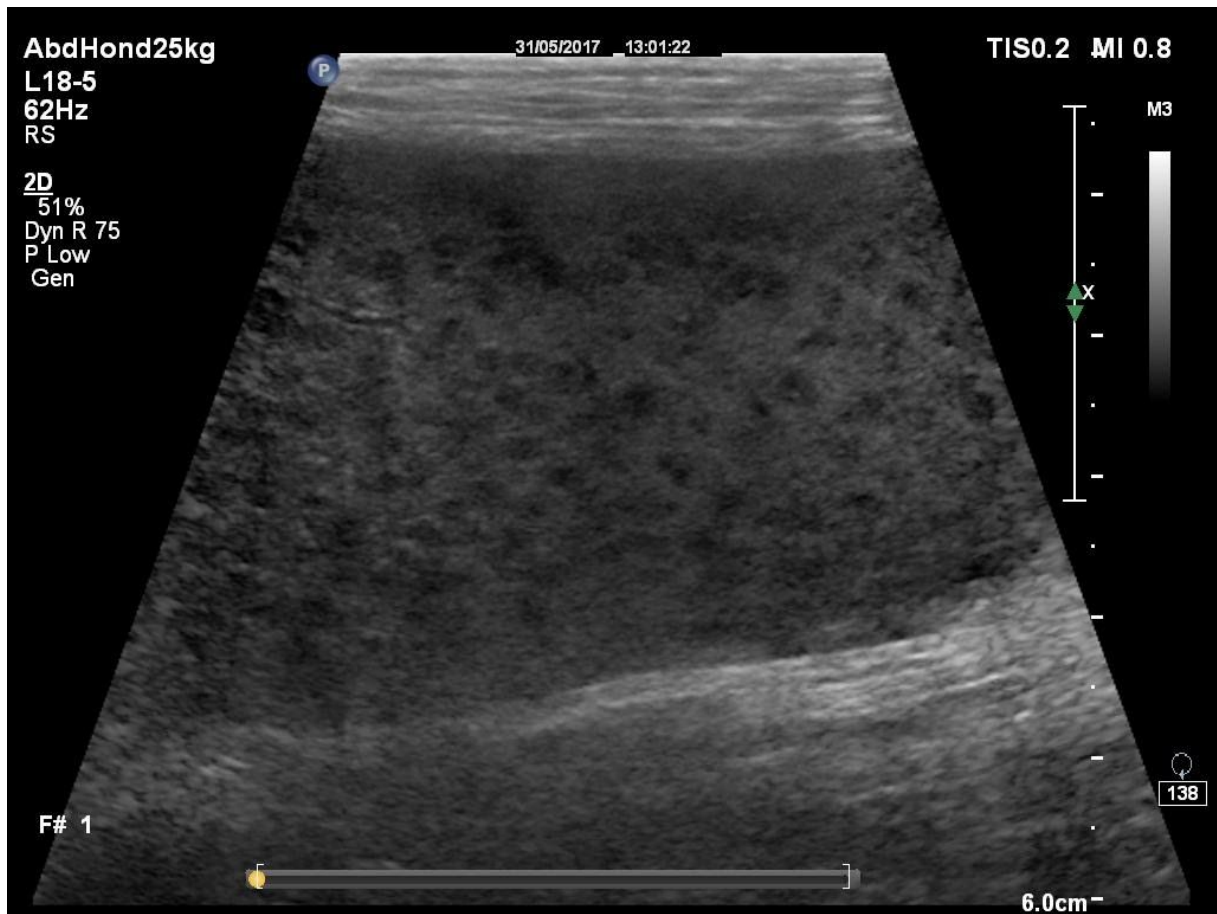
Sagittal image of the gallbladder. Normal oval to elongated shape, normal wall thickness. Some echogenic biliary sediment is present at the level of the gallbladder neck.

Transverse image of the liver, focused on the gallbladder. In the near field, the gallbladder contains a small amount of normal anechoic bile. Echogenic biliary sediment is present in the dependent portion of the gallbladder, without causing distal acoustic shadowing. Adjacent to the gallbladder, a small amount of peritoneal effusion can be detected.

Sagittal image of the body of the spleen at the level of the hilum. The splenic parenchyma is heterogeneous with hypoechoic nodules of variable size dispersed throughout the parenchyma. An anechoic splenic vein is seen in the middle of the image, branching into the spleen. A smooth hyperechoic, fine and well defined capsule is detected with a regular surface. Dorsal to the spleen the abdominal mesentery appears strongly hyperechoic.

Longitudinal view of the spleen. Using increased dynamic range results in a smoother image.

Sagittal image of the spleen showing a small hyperechoic and well demarcated nodule. Some of the smaller hypoechoic nodules appear to coalescence. The splenic capsule is fine, hyperechoic and smooth and the nodules do not protrude at the surface.

Transverse image of the spleen. Presence of numerous small hypoechoic nodules throughout the splenic parenchyma resulting in a motheaten pattern. A small amount of anechoic peritoneal effusion is detected adjacent to the spleen.

Transverse image of the stomach containing some fluid content. Normal wall layering, normal wall thickness. No abnormalities detected.

Longitudinal image of the descending duodenum. Normal wall thickness, normal layering, normal content. No abnormalities detected.

Transverse image of the duodenum showing normal wall thickness (0.47 cm between the calipers), normal layering, normal muscularis/mucosa ratio and a small amount of normal fluid content. The surrounding mesentery is diffusely hyperechoic.

Longitudinal and transverse section (between the calipers) of 2 jejunal loops. Normal wall thickness, normal layering and normal content.

Longitudinal image of the ileocolic junction. The ileum (right side) is entering the ascending colon (left side) which contains gas causing a distal acoustic shadowing. A transverse section through a jejunal loop is visible in the near field. No abnormalities detected.

Longitudinal view of the descending colon. Gas content is causing acoustic shadowing masking the colic wall in the far field and underlying structures. The colic wall has a normal layering although some increase in thickness is noted (0.249 cm between the calipers) according to reference values published by Penninck and d'Anjou.[16]

Transverse view of the caudal descending colon. The colic lumen is empty and the colon has collapsed, causing the wall to appear thickened. The colic folds are visible in this view. A hyperechoic band is present within the muscular layer and runs parallel to the serosal layer.

Longitudinal image of the left pancreatic limb. Normal shape, normal size, normal echogenicity and homogeneous pancreatic parenchyma. The surface is smooth and regular. Hyperechoic surrounding mesentery is present.

Longitudinal image of the left kidney. Normal shape, normal cortex and normal medulla. Renal size is within normal reference value.

Transverse image of the left kidney. No abnormalities detected.

Longitudinal image of the right kidney. The renal margins are ill-defined due to the hyperechoic and hyperattenuating abdominal fat.

Transverse image of the right kidney. No abnormalities detected.

Longitudinal image of the left adrenal gland. The caudal pole is indicated between the calipers (0.64 cm). A normal bilobed shape is detected and the thickness is within normal limits. No differentiation between cortex and medulla is seen. A transverse section through the phrenicoabominal vein is seen in the middle of the adrenal gland. Adjacent to the left adrenal gland, the aorta is demonstrated between the calipers (1.07 cm).
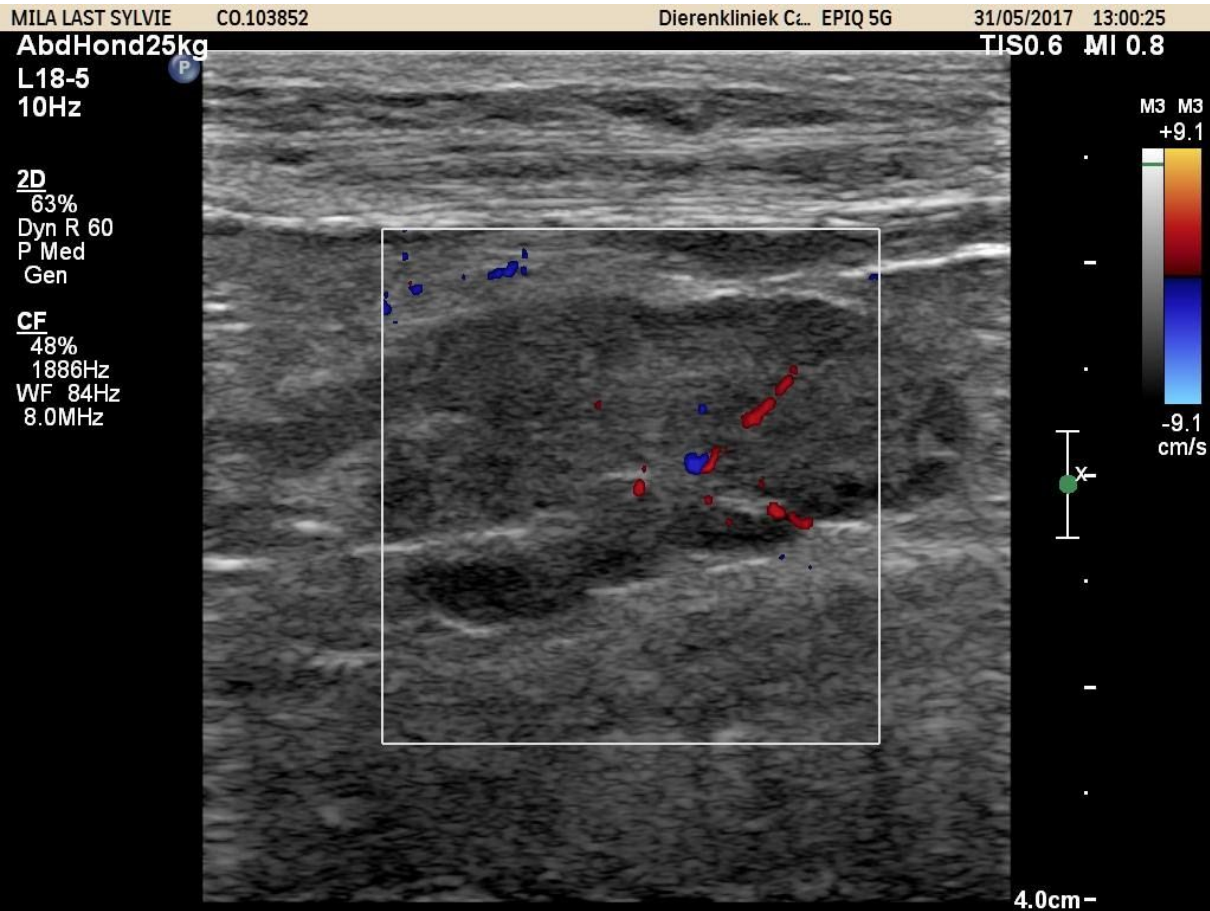
Longitudinal image of the right adrenal gland. Normal shape, normal size, normal internal structure. The caudal vena cava is seen as an anechoic structure adjacent to the adrenal gland. Near field: oblique view of the descending duodenum.
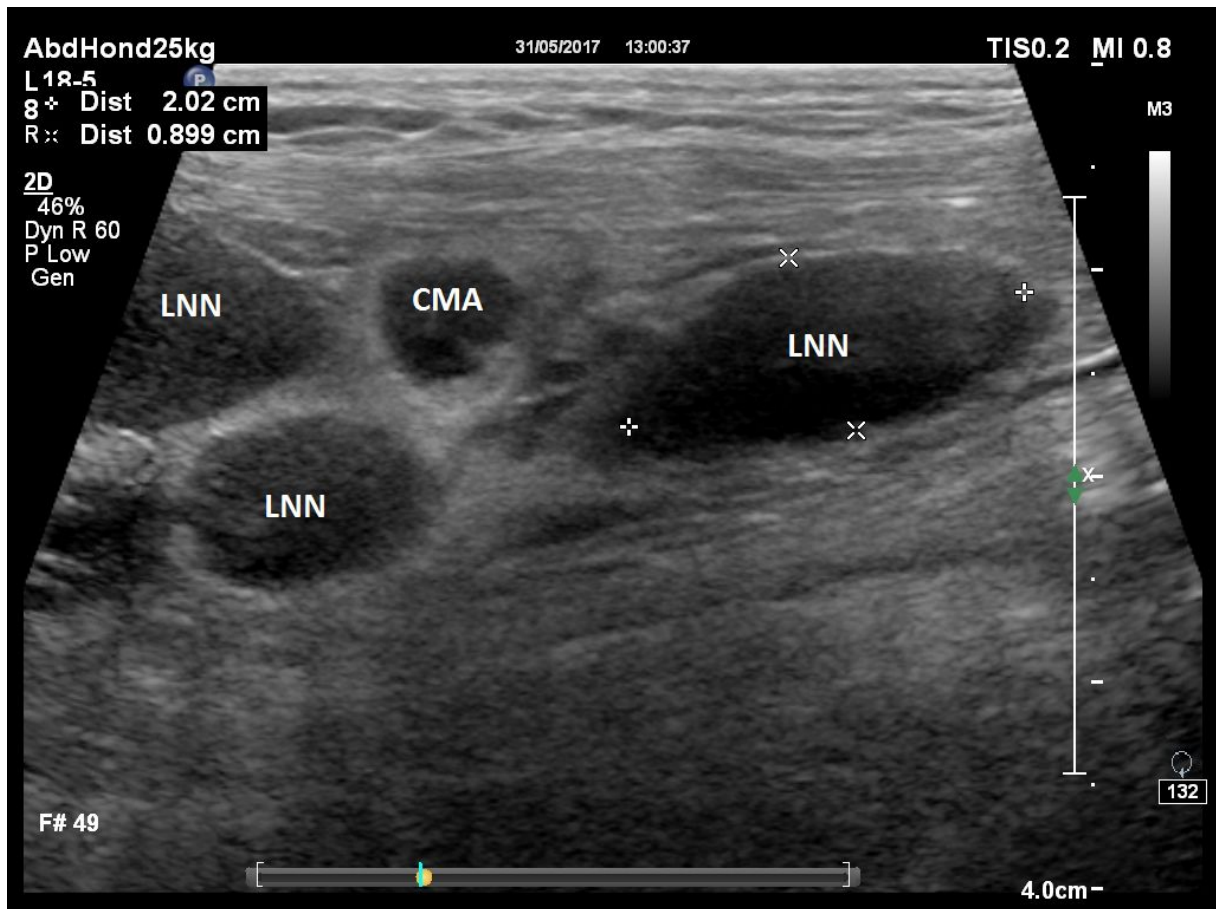
Longitudinal image of the urinary bladder. Normal shape, normal bladder wall thickness and layering. Moderate to large amount of normal anechoic intraluminal content is present. Intraluminal echogenicity is seen in the near field due to slice thickness artifact. A part of the beam is straddling the wall of the urinary bladder causing low energy echoes which are erroneously displayed within the lumen. This artifact is inherent to the beam width and disappears when the complete ultrasound beam is placed within the urinary bladder. Moving the focal zone upwards could improve the near field quality. This artifact is sometimes difficult to differentiate from secondary lobe artifacts (side-lobe and grating lobe artifacts) but the slice thickness artifact occurs in the "Z-plane" which is perpendicular to the scan plane and the ultrasound beam axis. The slice thickness artifact is caused by a reflector that is not seen in the image.
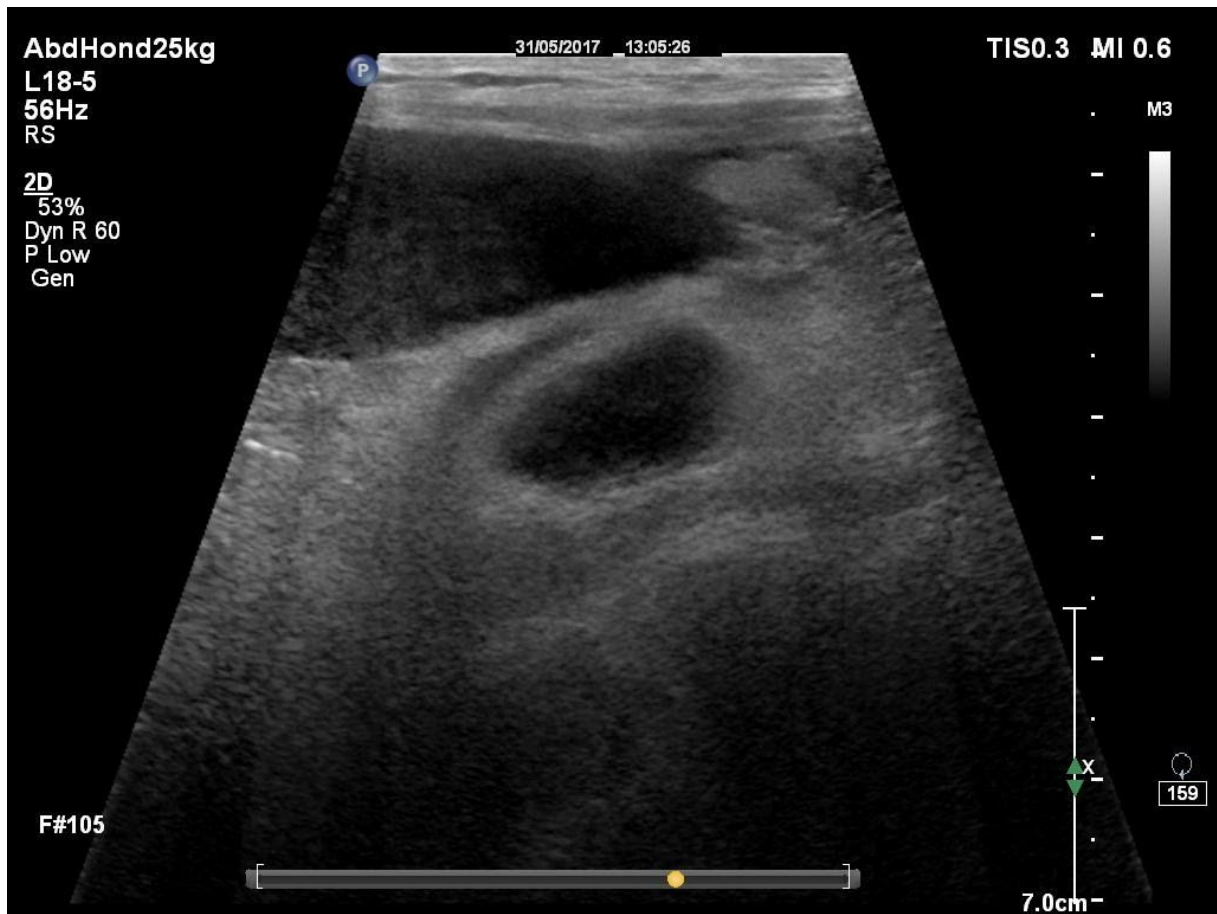
Longitudinal image of the left medial iliac lymph node. The lymph node is clearly hypoechoic to the surrounding abdominal fat. A normal fusiform shape is still recognizable although the lymph node is starting to become more round. The internal structure is homogeneous and a smooth surface is present. A short to long axis ratio of 0.26 is present, which is considered to be normal according to Penninck and d'Anjou.[16] A hypoechoic rim is seen at the dorsal side of the lymph node.

Color Doppler assessment of the right medial iliac lymph node showing a normal hilar vascularization. No increased blood flow at the periphery is noted.
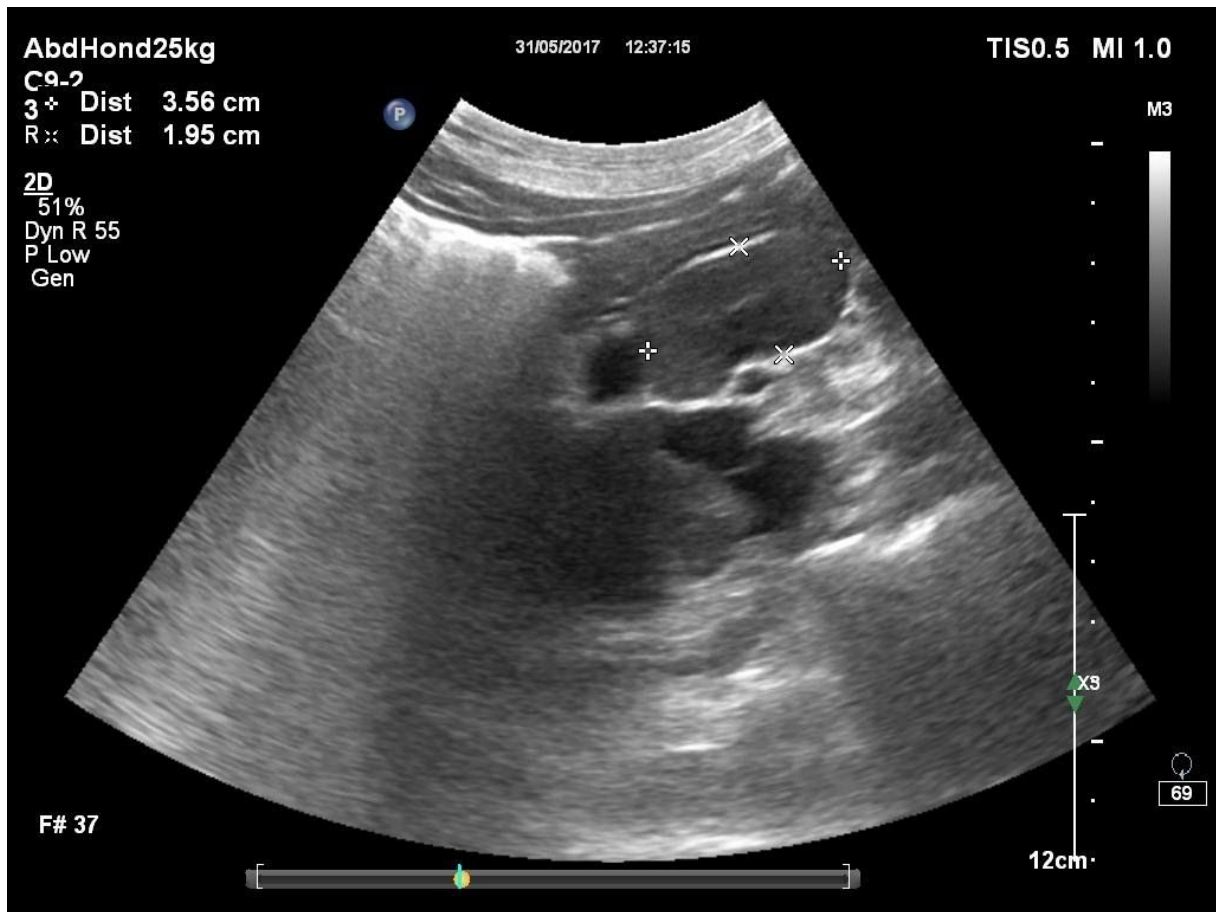
Longitudinal and transverse view of the jejunal lymph nodes (LNN). The jejunal lymph nodes are losing their fusiform shape and appear more rounded and diffusely hypoechoic. The internal structure is still homogeneous. The size of the lymph node indicated between the calipers is slightly increased when taking into account the reported reference values by Penninck and d'Anjou.[16] The jejunal lymph nodes are aligned around the cranial mesenteric artery (CMA). The surrounding mesentery has an increased echogenicity.

One of the aortic lymph nodes is detected and is clearly hypoechoic to the hyperechoic surroundings.

The splenic lymph node (measuring 1.24 to 1.78 cm between the calipers) is also clearly hypoechoic and enlarged and lies adjacent to the splenic vein. The stomach is seen on the left side of the image.

One of the hepatic lymph nodes (1.95 to 3.56 cm) is visualized, caudodorsally to the gastric body (near field) and adjacent to the portal vein (round anechoic structure). This lymph node is clearly enlarged although less hypoechoic when compared to the other abdominal lymph nodes. The left side of the image cannot be assessed due to acoustic shadowing caused by gastric intraluminal gas.

Fine needle aspiration of the spleen using a 23 Gauge needle.

Interpretation summary

The spleen has lost its fine and homogeneous echotexture, which is replaced by a honeycomb appearance with the presence of diffusely dispersed hypoechoic nodules. Some of the nodules appear to coalescence to larger lesions. The spleen is enlarged and the cranial and caudal poles are mildly rounded. The splenic capsule is seen as a thin and hyperechoic line and no nodules or masses are protruding at the surface. This "motheaten appearance" is most commonly seen with lymphoma although extramedullary haematopoiesis, infection and other neoplastic processes (especially other round cell tumors) need to be ruled out. One smaller hyperechoic and irregular lesion measuring 0.322 to 0.425 cm is detected in the spleen. Differential diagnosis include myelolipoma, haematoma, nodular hyperplasia, granuloma and neoplasia.[13,16]

The jejunal, medial iliac, portal, aortic and splenic lymph nodes are prominent and most of them show an increased spherical shape. The internal structure is still homogeneous although a diffuse hypoechogenicity is noted when compared to normal lymph nodes. The hypoechoic lymph nodes contrast well with the hyperechoic surroundings. They show a normal hilar vascularization and none of them has increased peripheral blood flow, which is reported by some authors as a sign of malignancy. The thin hyperechoic capsule is still visible and the surface is smooth. The jejunal lymph nodes measure 0.90 to 2.02 cm, which is mildly increased when using Penninck and d'Anjou reference ranges.[16] The left hepatic lymph node is prominent and appears enlarged although Pugh[17] reports normal left hepatic lymph nodes reaching up to 6 cm in length. Only one splenic lymph node is visualized in this patient, measuring 1.24 to 1.78 cm which is again within the reference ranges (0.5 to 4.0 cm) according to Pugh.[17] The right medial iliac lymph node is measuring 1.14 to 4.32 cm. Pugh[17] found normal medial iliac lymph nodes reaching up to 6 cm although maximal length described by Llabrés[12] is 4.0 cm, which classifies the medial iliac lymph node as enlarged. The short to long axis ratio of this lymph node is demonstrated (0.26) and is less than 0.5, as is described for normal lymph nodes by Penninck and D'Anjou.[16] The remaining abdominal lymph nodes could not be visualized.

The gallbladder has a normal shape, normal wall thickness and contains some echogenic sludge at the level of the gallbladder neck, in the dependent portion. This sludge is reported in association with a delayed gallbladder emptying and is seen in cases with cholestasis. Predisposition to development of a gallbladder mucocoele or other gallbladder pathologies is unknown.[19]

The colic wall shows a mild increased thickness, measuring 0.25 cm. Diffuse and circumferential colic wall thickening with preservation of layering is mostly associated with inflammatory (lymphoplasmocytic/eosinophilic), infectious (parasitic) or immune-mediated disease. Neoplastic disease – and especially lymphoma – may cause similar changes. A white hyperechoic band is present within the muscular layer of the colon and runs parallel to the serosal layer. This sonographic appearance has been reported to be associated with the presence of fibrous tissue within the myenteric plexus.[8]

The mesentery is increased in echogenicity and a small amount of anechoic peritoneal effusion is detected in the four quadrants. The hyperechogenicity of the abdominal fat is sometimes pronounced due to overgaining, especially in the images made with the linear probe.
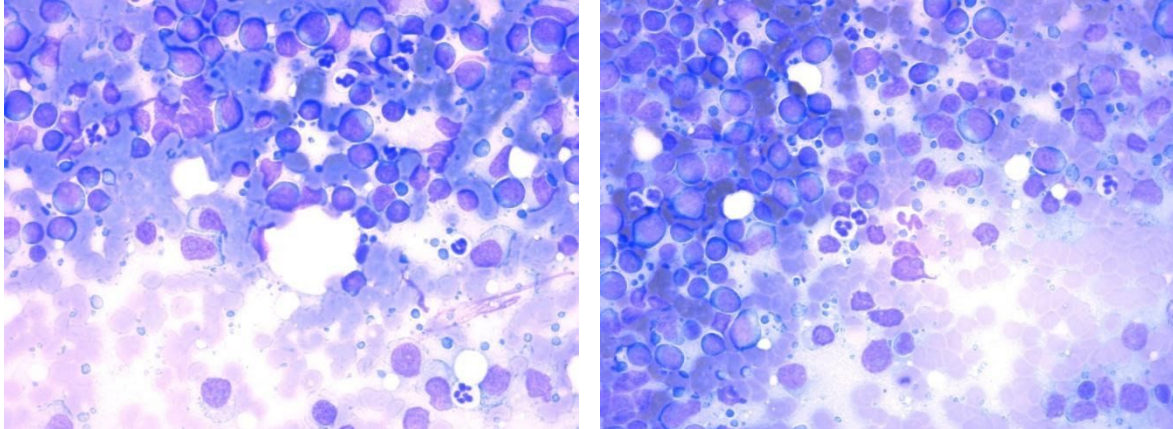
A 23G needle is used for fine needle aspiration of the spleen (3 samples), the liver (1 sample) and the jejunal lymph nodes (1 sample). One milliliter of the abdominal fluid is sampled, which is clear.

<u>Conclusion</u>:

Moderate splenomegaly with rounding of the margins and dispersed multifocal small hypoechoic nodules resulting in a honeycomb appearance of the spleen. Increased size and hypoechogenicity of most of the abdominal lymph nodes and a small amount of abdominal effusion is present. These sonographic changes are most compatible with lymphoma.

The cytology of the spleen, liver and lymph nodes are assessed in clinic and are strongly suspected of lymphoma. One splenic sample, jejunal lymph node sample and the fine needle aspiration of the left prescapular and right popliteus lymph node are sent to an extern lab for confirmation. Since previous samples taken by the referring veterinarian were non diagnostic, biopsies of the mandibular lymph nodes are taken. The thoracic radiograph is not repeated as the owners only ask for a diagnosis and do not wish to further stage the disease if lymphoma is ultimately diagnosed. As chemotherapy is not an option for the owners, Mila is started on corticosteroids at a dosage of 1 mg/kg twice a day, combined with omeprazole 20 mg once a day. Optimmune Canis® (cyclosporine A) is used as a topical ointment for treatment of the keratoconjunctivitis sicca as it inhibits proliferation of cytotoxic T-cells and T-helper cells in the lacrimal gland, resulting in increased tear production.
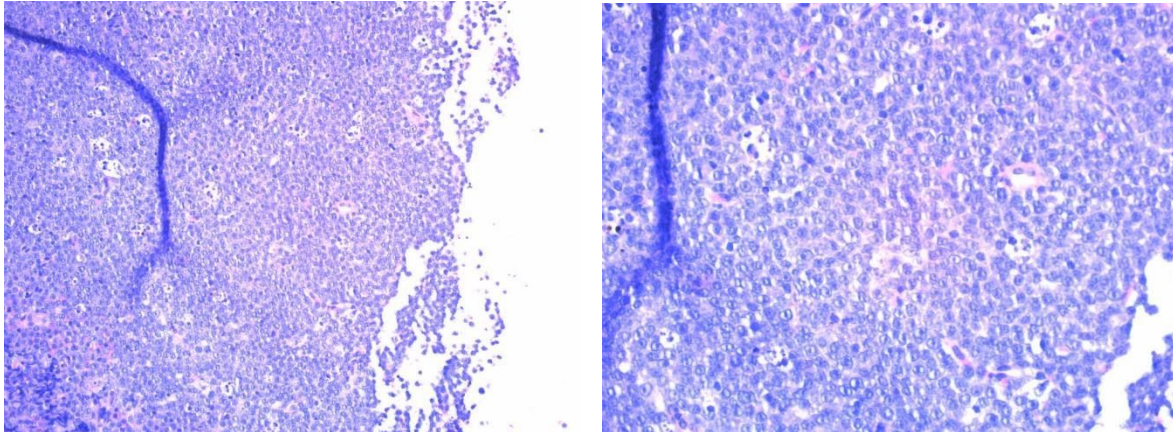
Cytology

All samples (with the exception of the peritoneal fluid) are highly cellular with moderate preservation of the cellular structure, due to superimposition and frequent loss of cytoplasm. The samples of the spleen show a predominantly lymphoid cell population with mostly large lymphocytes containing a mild basophilic cytoplasm and a centrally located round nucleus. The nucleus has a regular nuclear membrane and finely granulated chromatin pattern with multiple and prominent centrally located nucleoli, which are varying in size. Some mitotic figures are present. Small lymphocytes are present and quite an amount of neutrophils, macrophages and some eosinophils are seen as well.

The samples for the subscapular and popliteus lymph nodes show analogous large lymphocytes.

The abdominal effusion contains a heterogeneous cell population with the presence of small and large lymphocytes, neutrophils, and some mesothelial cells.

Fine needle aspiration of the mandibular lymph node and liver were examined in clinic. The liver sample had the same population as seen in the spleen. Normal hepatocytes were present as well. The mandibular lymph node consisted of large lymphocytes.

Histopathology

Lymph node: several sections were assessed which showed loss of normal architecture due to the presence of large lymphocytes. These lymphocytes contain a limited amount of ill-defined eosinophilic cytoplasm and a rounded centrally located nucleus with granular chromatin pattern and one or more prominent centrally located nucleoli. Mitotic figures are detected (mitotic index: 8). Debris-laden macrophages are numerous. Multifocal haemorrhage is present.

Locally, perinodal fat tissue is visible which is infiltrated by neoplastic cells. Additionally, a salivary gland fragment is found which is also diffusely infiltrated with neoplastic cells.

Conclusion:

Diffuse large cell and high grade lymphoma with infiltration in the adjacent fat tissue and salivary gland. Additional immunohistochemical typing is recommended.

Case discussion

Lymphoma is the most common haematopoietic neoplastic disorder in dogs and is caused by a clonal proliferation of lymphocytes.[4,5,6,9,14,21] The incidence of canine lymphoma is increasing, as is in human medicine.[21] Larger breeds are overrepresented including Boxer dogs, Dobermanns, English Bulldogs, Labrador Retrievers, Golden Retrievers, Bassets and German Shepherds.[2,4,14,21] Familial predilection has been reported in Rottweilers, Bullmastiffs, Otter hounds and Scottish Terriers.[9,21] Middle-aged to older dogs are most commonly affected.[4,6,9,14,21] Generally, no sex predisposition is known for canine lymphoma[9,21], although some report overrepresentation of male dogs[4,14] or lower prevalence in intact females.[21] In Golden Retrievers, early neutering was found to be associated with increased incidence of lymphosarcoma.[21] No causative agent has been demonstrated although viral infections, immune-mediated factors, chemicals, magnetic fields, radioactivity and pollution have been demonstrated to increase the risk for developing lymphoma.[6,14,21] Genetic predisposition has been described and Golden Retrievers with lymphoma were found to have a defective DNA repair mechanism when compared to healthy patients.[6,21]

The multicentric form, involving the peripheral lymph nodes, is the most common presentation and accounts for 75% of all canine lymphomas.[4,5,6,14,21] Besides the lymph nodes, other organs can be affected too including the gastrointestinal tract, liver, spleen, kidney, eye, skin, central nervous system, and lungs.[4,6,14,21] Multicentric lymphoma is classified by the World Health Organization into five stages. Stage I includes dogs with involvement of a single lymph node. Stage II in case of regional lymph node involvement. Stage III is the generalized lymphadenopathy. Stage IV when liver and / or spleen are involved and stage V includes blood and/or bone marrow involvement.[2,21] Subclassification in substage a indicates the absence of systemic signs and substage b is associated with clinical disease.[4,14,21] Symptoms associated with multicentric lymphoma include generalized lymphadenopathy, splenomegaly, decreased appetite, fever, weight loss, vomiting/diarrhea, respiratory problems and hepatomegaly.[6,10,14,21] According to the WHO Mila is classified as a stage IV (at least), substage b.

Thoracic radiography, abdominal radiography, haematology and chemistry profiles are mostly normal or show nonspecific changes.[4,6,14,21] Hypercalcemia is sometimes present as a paraneoplastic syndrome and is mostly associated with T-cell lymphoma, although similar prevalence in B-cell lymphoma is reported by others.[6,21] Other syndromes are monoclonal gammopathy, hypoglycemia and immune-mediated diseases.[21]

Ultrasonographic examination

Ultrasound is a useful tool in assessing splenic, hepatic and abdominal lymph node involvement, although 25 % will show no sonographic changes.[21]

Splenic lymphoma may show a variety of appearances and can present as one focal mass or multifocal nodules of varying size and echogenicity, with smooth splenic margins or with masses protruding at the surface.[2,11,13,16] These nodules cannot be differentiated from nodular hyperplasia, extramedullary haematopoiesis, fibrous histiocytic nodules, amyloidosis, splenitis, haematoma and other infiltrative neoplastic disease based on ultrasound alone.[13,16] Internal cavitation of the mass may be seen and in some cases lymphoma is detected as a target lesion.[11,13] Abdominal effusion may be detected[2], as seen in Mila's case. The typical Swiss-cheese appearance or also called honeycomb

or motheaten spleen, is characterized by the presence of diffuse dispersed and often ill-defined small hypoechoic nodules throughout the splenic parenchyma.[2,16,21] In splenic lymphoma, a sensitivity of 100% for detecting ultrasonographic changes has been reported. However, specificity is low being 23.3%. A positive predictive value of 64.7% and a negative predictive value of 100% has been described. Consequently, sampling an ultrasonographic normal spleen for detection of lymphoma is of little use. In case the patient presents with a motheaten splenic appearance, the positive predictive value is even increased to 100%.[2] In Mila's case however additional histopathology was required by the histopathologist because of long lasting concurrent infection. Another study reported a sensitivity of 83.33% for detecting splenic involvement in a small group (5 patients) consisting of dogs and cats.[11] This is exactly the same number reported by Hanson et al[7], a study consisting of 30 cats with splenic lymphosarcoma.[7] Overall, fine needle aspiration of splenic lesions for the diagnosis of lymphoma is relatively low as specificity is only 23.3% and is associated with a high number of false positives.[1,2] Ballegeer et al[1] found that differentiating lymphoma from reactive lymphoid hyperplasia is difficult and 31% of the neoplastic diseases were missed during cytological examination. The negative prognostic value is high, indicating that cytology sampling of a normal ultrasonographic appearance is not likely to provide additional information.[1,2]

The sonographic features of hepatic lymphoma varies between diffuse hypoechogenicity, hyperechogenicity, hypoechoic nodules and target lesions with or without hepatic enlargement. In some cases, as in Mila's case, no ultrasonographic abnormalities are detected.[2,11,13,16] Sensitivity and specificity for detecting sonographic hepatic changes in dogs with lymphosarcoma was found to be 72.7% and 77.4% respectively, indicating ultrasound can be used to screen for liver involvement in this disease. A positive predictive value of 77.4% and a negative predictive value of 76.3% was found.[2] A similar sensitivity (68%) is reported by Warren-Smith.[20] However, lower rates have been published by others. Lamb et al found[11] a striking low sensitivity of 10% for detecting hepatic lymphosarcoma in dogs. In cats, a sensitivity of 40% was reported.[11] The significant difference between both studies may be due to the fact that both studies compromise only a small population size. A difference of 19 years is present between Crabtee[2] and Lamb[11], and improvement of ultrasound equipment may also explain the higher sensitivity and specificity in more recent studies.

The abdominal lymph nodes should be isoechoic to slightly hypoechoic to the adjacent mesentery. They have a fusiform to oval shape, fine homogeneous echotexture and smooth surroundings.[15,16,17] Internal heterogenicity is mostly associated with malignancy although this can also be seen in inflammatory disease.[10] Neoplastic lymph nodes are usually enlarged, clearly hypoechoic and show rounded edges.[3,10,15,16] Mila's abdominal lymph nodes also show these sonographic features. A short to long axis ratio of less than 0.5 is considered to be normal, although this measurement is only described for medial iliac and superficial inguinal lymph nodes.[3,16] The detection of a high number of abdominal lymph nodes is usually associated with neoplastic disease.[12] Some authors report internal mineralization, peripheral oedema and sharp irregular delineation in case of malignancy.[3,12,15,20] Peripheral and mixed vascularization instead of hilar blood is described as a malignant feature in lymph nodes although this has been refuted by others.[3,10,15] Invasion of the adjacent blood vessel may be seen. However, even when considering all these ultrasonographic characteristics, differentiation between malignant and benign processes cannot be done based on ultrasound alone.[12]

As described above, cytology is a sensitive and quick diagnostic method for diagnosing canine lymphoma although histopathology is often necessary for confirmation and mandatory for staging.[21] The majority of canine lymphomas belong to the diffuse and intermediate to large cell lymphomas.[18]

Prognosis

Some authors report no influence of age, weight or gender on chemotherapy treatment[5], others report a better outcome for young and male dogs.[9] Female dogs and small breeds with stages I-IV and substage a were demonstrated to have a better prognosis,[21] although this is refuted by other authors.[5] Negative prognostic indicators include hypercalcemia, presence of chronic inflammatory process, T-cell phenotype and pretreatment with corticosteroids, which all result in shorter remission times and decreased survival times.[5,6,14,21]

Therapy

Chemotherapy is still the gold standard for treatment of lymphoma in dogs. Many different protocols ranging from 12 weeks to 2 years have been described.[18,21] Combination chemotherapies are associated with better results when compared to single-agent therapy and include combinations between doxorubicin, cyclophosphamide, vincristine, L-asparaginase, and prednisolone.[14,21] CHOP protocols are mostly used as induction therapy and are reported to have the highest response rate.[18,21] Many variations of the CHOP protocol have been investigated, all resulting in similar complete response rates (between 60 and 90%) and similar mean survival times (between 6 and 9 months).[4,6,14,18] Single agent therapy is also available with doxorubicin as being the most popular and effective one, but L-asparaginase, mitoxantrone and CCNU may also be used. Untreated multicentric lymphoma is associated with an expected survival time of 1 to 2 months, which is similar to treatment with prednisolone only.[14,21]

References

1. Ballegeer EA et al (2007). Correlation of ultrasonographic appearance of lesions and cytologic and histologic diagnoses in splenic aspirates for dogs and cats: 32 cases (2002-2005). *J Am Vet Med Assoc* 230, pp 690-696

2. Crabtree AC et al (2010). Diagnostic accuracy of gray-scale ultrasonography for the detection of hepatic and splenic lymphoma in dogs. *Veterinary Radiology & Ultrasound* Vol.51, No.6, pp 661-664

3. De Swarte M et al (2011). Comparison of sonographic features of benign and neoplastic deep lymph nodes in dogs. *Veterinary Radiology & Ultrasound* Vol.52, No.4, pp 451-456

4. Dobson JM and Gorman NT (1993). Canine multicentric lymphoma. 1: Clinicopathological presentation of the disease. *Journal of Small Animal Practice* 34, pp 594-598

5. Dobson JL et al (2001). Prognostic variables in canine multicentric lymphosarcoma. *Journal of Small Animal Practice* 42, pp 377-384

6. Gavazza A et al (2009). Clinical, laboratory, diagnostic and prognostic aspects of canine lymphoma; a retrospective study. *Comp Clin Pathol* 18 (3), pp 291-299

7. Hanson JA et al (2001). Ultrasonographic appearance of splenic disease in 101 cats. *Veterinary Radiology & Ultrasound* Vol. 42, No.5, pp 441-445

8. Heng GH et al (2015). Prevalence and significance of an ultrasonographic colonic muscularis hyperechoic band paralleling the serosal layer in dogs. *Vet Radiol Ultrasound* Vol.56, No.6, pp 666-669

9. Jagielski D et al (2002). A Retrospective Study of the Incidence and Prognostic Factors of Multicentric Lymphoma in Dogs (1998-2000). *J Vet Med* A49, pp 419-424

10. Kinns J and Mai W (2007). Association between malignancy and sonographic heterogeneity in canine and feline abdominal lymph nodes. *Veterinary Radiology & Ultrasound* Vol.48, No.6, pp 565-569

11. Lamb CR et al (1991). Ultrasonographic findings in hepatic and splenic lymphosarcoma in dogs and cats. *Veterinary Radiology* Vol.32, No.3, pp 117-120

12. Llabrés-Diaz FJ (2004). Ultrasonography of the medial iliac lymph nodes in the dog. *Veterinary Radiology & Ultrasound* Vol.45, No.2, pp 156-165

13. Mattoon JS and Nyland TG (2015). Small Animal Diagnostic Ultrasound (third edition). Saunders, an imprint of Elsevier Inc, Missouri, p 348-355, 400-437

14. Mortier F et al (2012). Canine lymphoma: a retrospective study (2009-2010). *Vlaams Diergeneeskundig Tijdschrift* 81, pp 341-351

15. Nyman HT and O'Brien RT (2007). The Sonographic Evaluation of Lymph Nodes. *Cln Tech Small Anim Pract* 22, pp 138-137

16. Penninck D and d'Anjou MA (2015). Atlas of Small Animal Ultrasonography (second edition). John Wiley & Sons, Inc, pp 239-258, p 197,

17. Pugh CR (1994). Ultrasonographic examination of abdominal lymph nodes in the dog. *Veterinary Radiology & Ultrasound* Vol.35, No.2, pp 110-115

18. Regan RC et al (2012). Diagnostic evaluation and treatment recommendations for dogs with substage a high-grade multicentric lymphoma: results of a survey of veterinarians. *Veterinary and Comparative Oncology* 11(4), pp287-295

19. Tsukagoshi T et al (2012). Decreased gallbladder emptying in dogs with biliary sludge or gallbladder mucocoele. *Veterinary Radiology & Ultrasound* Vol.53, No.1, pp 84-91

20. Warren-Smith CMR et al (2012). Lack of associations between ultrasonographic appearance of parenchymal lesions of the canine liver and histological diagnosis. *Journal of Small Animal Practice* Vol.53, pp 168-173

21. Zandvliet M (2016). Canine Lymphoma: a review. *Veterinary Quaterly* 36(2), pp 76-104